Available online at www.sciencedirect.com

ScienceDirect

Ceramics International 39 (2013) 9003–9008

CERAMICS INTERNATIONAL

www.elsevier.com/locate/ceramint

Chemical synthesis of TiO_2 nanoparticles and their inclusion in Ni–P electroless coatings

Preeti Makkar*, R.C. Agarwala, Vijaya Agarwala

Department of Metallurgical and Materials Engineering, Indian Institute of Technology Roorkee, Roorkee 247667, India

Received 16 April 2013; received in revised form 27 April 2013; accepted 28 April 2013
Available online 18 May 2013

Abstract

The work addresses the preparation of Ni–P–TiO_2 nanocomposite coatings on mild steel substrate by the electroless technique. Nanosized TiO_2 particles were first synthesized by the precipitation method and then were codeposited (4 g/l) into the Ni–P matrix using alkaline hypophosphite reduced EL bath. The surface morphology, particle size, elemental composition and phase analysis of as-synthesized TiO_2 nanoparticles and the coatings were characterized by field emission scanning electron microscopy (FESEM), energy-dispersive analysis of X-ray (EDAX) and X-ray diffraction (XRD). Coatings with 20 μm thickness were heat treated at 400 °C for 1 h in argon atmosphere. The morphology, microhardness, wear resistance and friction coefficient characteristics (ball on disc) of electroless Ni–P–TiO_2 nanocomposite coatings were determined and compared with Ni–P coatings. The results show that as-synthesized TiO_2 nanoparticles are spherical in shape with a size of about12 nm. After heat treatment, the microhardness and wear resistance of the coatings are improved significantly. Superior microhardness and wear resistance are observed for Ni–P–TiO_2 nanocomposite coatings over Ni–P coatings.

Keywords: C. Wear resistance; Electroless (EL); Ni–P–TiO_2; Microhardness; Precipitation

1. Introduction

Electroless (EL) Ni–P coating is one of the reliable and efficient surface engineering technologies used in industries to improve the physical and mechanical properties due to its uniform deposition, excellent wear and corrosion resistance. [1]. Embedding various soft/hard particles into the Ni–P matrix can further enhance the surface properties and thus EL composites have attracted much attention [2–5]. It is believed that titania (TiO_2) due to its excellent mechanical properties is used as the second phase for improving the hardness and wear resistance of Ni–P coating. Therefore, the EL Ni–P–TiO_2 nanocomposites have extensively been explored for several technological applications [6,7]. Most EL composite studies focus upon the incorporation of micron sized second phase particles into the Ni–P matrix to yield better engineering properties [2–9]. The tribological studies on nanosized TiO_2 particles reinforced EL Ni–P matrix composite plating are limited till date [10,11].

However, the studies on reinforcement of nanosized titania particles prepared by precipitation into an EL Ni–P matrix are not reported till date. In the present approach, for the development of EL Ni–P–TiO_2 nanocomposite coatings, the embedded second phase nanosized TiO_2 particles are first synthesized by the precipitation method and then codeposited with Ni–P on the surface of mild steel. The morphology, phase changes and performance in terms of hardness and wear resistance of the Ni–P–TiO_2 nanocomposites with respect to Ni–P alloy were investigated.

2. Experimental

2.1. Synthesis of TiO_2 nanopowder/electroless Ni–P/Ni–P–TiO_2 coatings

The TiO_2 powder was synthesized using titanium trichloride ($TiCl_3$, Sigma-Aldrich) as the precursor and ammonia solution

*Corresponding author. Tel.: +91 741755393; fax: +91 1332285739.
E-mail address: pritty02@gmail.com (P. Makkar).

0272-8842/$ - see front matter © 2013 Elsevier Ltd and Techna Group S.r.l. All rights reserved.
http://dx.doi.org/10.1016/j.ceramint.2013.04.101

(NH_4OH, Merck) as the precipitating agent. $TiCl_3 \cdot 8H_2O$ (50 ml) was placed into a flask and the aqueous solution of concentrated ammonia solution (40 mL) was mixed in 25 mL of distilled water and then added dropwise to the flask containing $TiCl_3$ solution under continuous stirring at room temperature. The dark blue precipitates were observed and was aged under stirring for 16 h during which the color of the dispersion turned to white (pH 8.5) [12]. The precipitates were filtered and washed repeatedly with distilled water followed by washing with ethanol to remove all the chloride ions and dried in air at 100 °C. The dried powder was milled at 200 rpm for 4 h with ball to powder weight ratio 5:1 using high energy planetary ball mill. The milled powder was then calcinated in air at 500 °C for 1 h. Mild steel substrates (2.5 mm × 2.5 mm × 2 mm) were used for plating EL Ni–P alloy and Ni–P–TiO_2 nanocomposite coatings. Substrates were sensitized by 0.1% stannous chloride and activated by 0.01% freshly prepared palladium chloride solution. The plating bath contains nickel sulfate 30 g/l as a source of nickel ions, sodium hypophosphite 20 g/l as a reducing agent, sodium tri-citrate 100 g/l as a complexing agent, ammonium sulfate 50 g/l and ammonium chloride 50 g/l as stabilizers. The as-synthesized TiO_2 powder (4 g/l) was suspended in prepared EL bath by continuously stirring after the immersion of activated substrate into the bath. The bath maintained at pH 9.0, temperature 90 °C and plating time is 30 min. After plating, the samples were taken out, rinsed with deionized water and air dried.

2.2. Characterization

Thermal analysis of the dried TiO_2 powder was carried out using TG/DTA (Perkin-Elmer Diamond) in air at a heating rate of 10 °C/min. The phases of TiO_2 powder, Ni–P and Ni–P–TiO_2 coatings were determined by X-ray diffraction (XRD) (D8 Bruker AXS diffractometer) with Cu Kα target. Crystallite size was calculated by the Scherrer formula ($d = 0.9\lambda/\beta \cos\theta$) where d = crystallite size. The surface morphology of coatings and the powder were carried out by a field emission scanning electron microscope, FESEM (Quanta FEI-200) and a scanning electron microscope, SEM (ZEISS EVO-18). The compositional analysis of the coatings was carried by Energy dispersive
X-ray spectroscopy, EDAX (PENTA FET Precision). The particle size of the synthesized TiO_2 powder was confirmed by a transmission electron microscope, TEM (TECNAI G^2-20). Heat treatment was carried out in argon atmosphere at 400 °C for 1 h to improve the mechanical properties of Ni–P and Ni–P–TiO_2 coatings. The microhardness (VHN) of Ni–P and Ni–P–TiO_2 composite coatings was determined (make Future-Tech Corporation) on the surface of as-plated and HT specimens under a 10 gf load with dwelling time of 15 s. Hardness value was measured as an average of three measurements. Ball on disc tests were used to determine the coefficient of friction and wear resistance of the coatings. The mild steel discs with 42 mm diameter and 3 mm thickness were used against chromium steel ball of hardness 65 HRC. The disc was hardened by heating at 400 °C for 1 h in argon atmosphere. Wear tests were carried out at a sliding speed of 0.1and 0.2 m/s, temperature of 29 °C, 40% moisture, under 0.1, 0.15 and 0.20 N loads and 800 m sliding distance.

3. Results and discussion

The differential thermal analysis (DTA) curve [Fig. 1] of dried TiO_2 powder has the endothermic peak at 303 °C at a rate loss of 2.15 J/mg of energy. The TG trace of dried TiO_2 powder shows the weight loss of near about 69% between temperatures 200 °C and 220 °C, which indicates the evaporation of retained chlorine which can also be confirmed from XRD analysis [Fig. 4a]. Also an exothermic peak is observed at 470 °C which infers the anatase crystallite transformation. Thus, calcination of TiO_2 powder at 500 °C for 1 h results in the transformation to anatase phase of titania.

TEM and SEM micrograph reveals the morphology and the size range of calcinated TiO_2 powders at 500 °C [Fig. 2a and b]. The particles have the aspect ratio of ~1 and are agglomerated.

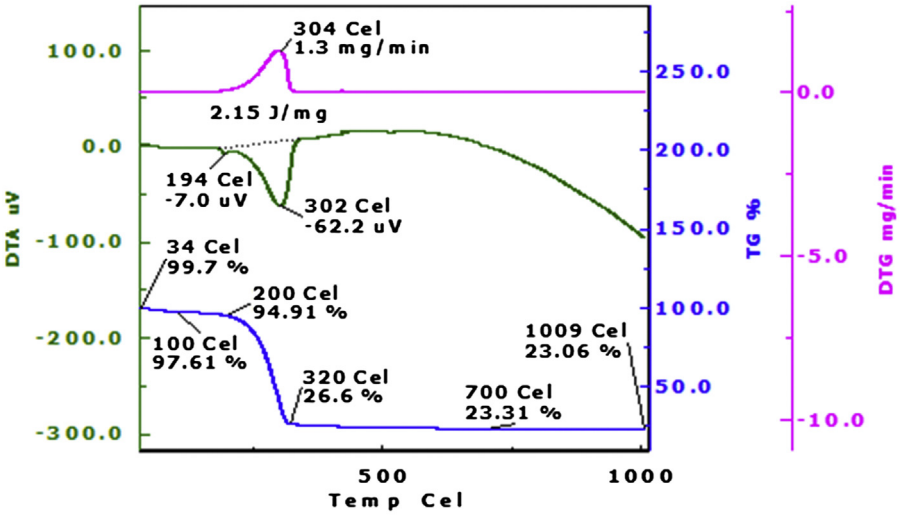

Fig. 1. DTA/TG traces of dried TiO_2 powder from room temperature to 1500 °C.

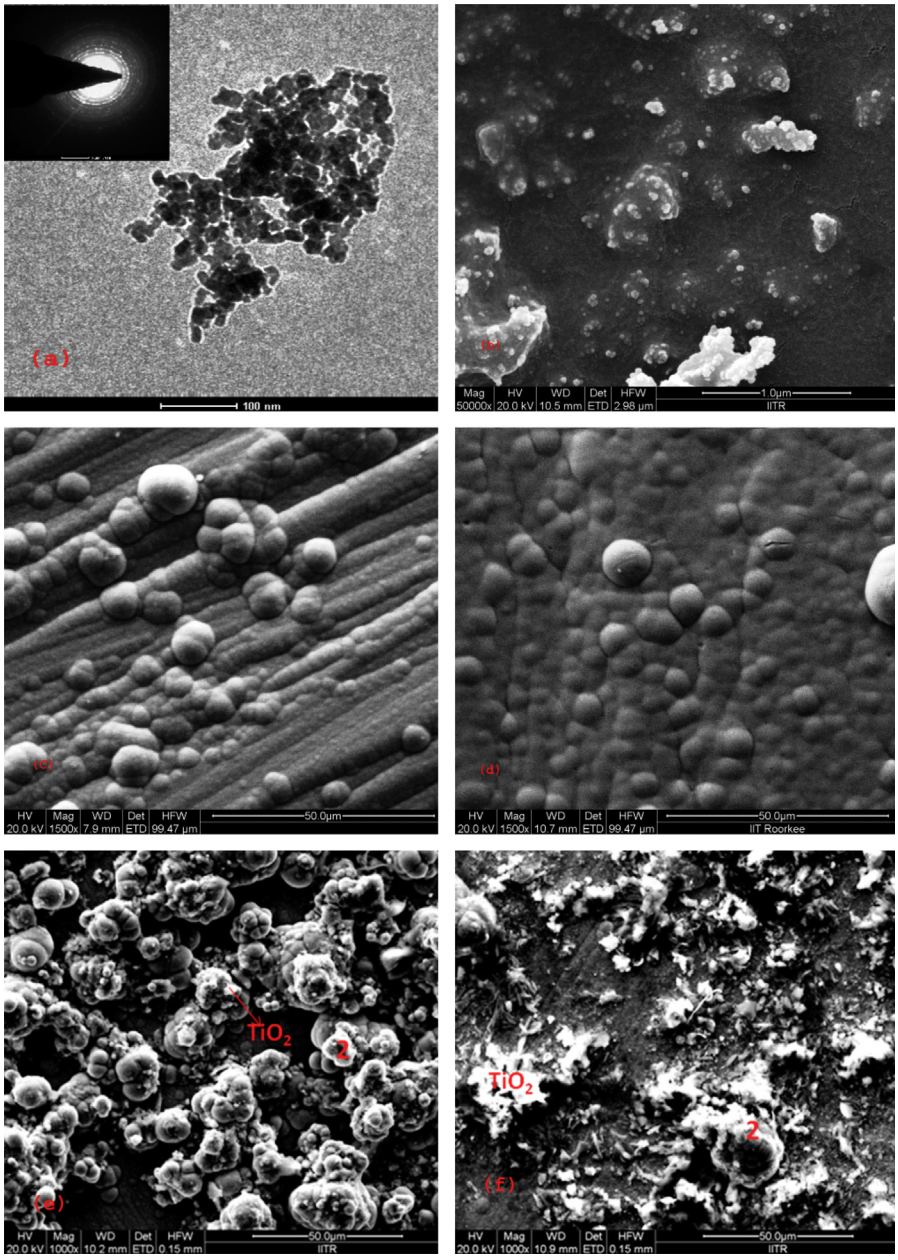

Fig. 2. TiO_2 powder examined under (a) TEM with SAD pattern, (b) FESEM; FESEM micrographs of EL coating, (c) Ni–P, (d) Ni–P HT, (e) Ni–P–TiO_2 and (f) Ni–P–TiO_2 HT.

SAD pattern confirms the presence of TiO_2. TEM results also confirmed the crystallite size of TiO_2 powder is about 12 nm. Ni–P alloy coating shows a globular structure [Fig. 2c] with average globular size of ~20 μm was observed having lateral growth followed by vertical growth. Heat treatment (HT) at 400 °C for 1 h in argon atmosphere results in flattering of globules thus the globule seems to be relatively coarser than Ni–P alloy coating [Fig. 2d and f]. It was observed that heat treatment hardly influence on surface topography. FESEM micrograph of EL Ni–P–TiO_2 nanocomposite coating is shown in Fig. 2e. The TiO_2 particles are seen on the Ni–P globules and in certain region, the particles are seen to be coated with Ni–P (region 2). The TiO_2 particles entrapment in the Ni–P globules is further confirmed by EDAX analysis [Fig. 4]. It can also be observed that surface of Ni–P–TiO_2 shows many nodular protrusions as compared with smooth surface of Ni–P alloy coating. These nodules are of spherical shape and compositional analysis [Fig. 3a] explains the presence of TiO_2 particles apart from nickel and phosphorus on nodules. The thickness of the coatings as measured by cross sectional analysis [Fig. 3b] is found to be around 20 μm.

The X-ray diffraction pattern of dried TiO_2 powder shows ammine titanium chloride phase as per JCPDS Ref. no.: 01-074-0508 [Fig. 5a]. After mechanical milling of dried TiO_2 powder for a period of 4 h, anatase phase of TiO_2 with lesser intensity is observed in the XRD pattern due to the heat generated by milling. XRD pattern of TiO_2 powder calcinated at 500 °C for 1 h [Fig. 5a] shows pure anatase phase of TiO_2

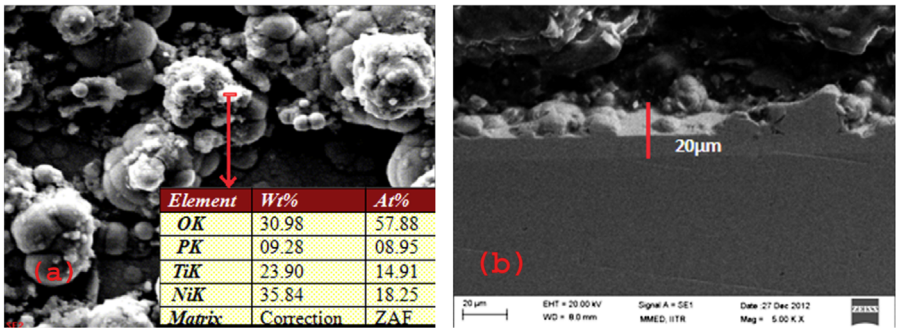

Fig. 3. Ni–P–TiO_2 nanocomposite coating (a) surface morphology with EDAX analysis under FESEM and (b) SEM micrograph showing cross section of heat treated coating.

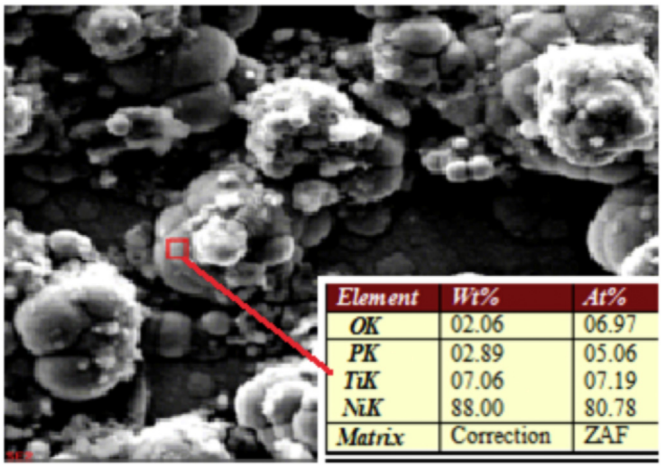

Fig. 4. Surface morphology with EDAX analysis of Ni–P–TiO_2 nanocomposite coating showing particle entrapment.

(JCPDS Ref. no.: 01-071-1166). The crystalline size of the calcinated powder calculated by the Scherer formula is about 12 nm which is further confirmed by TEM studies. XRD studies of EL Ni–P alloy coating [Fig. 5b] show a single broad peak which corresponds to microcrystalline nickel, Ni (JCPDS Ref. no.: 00-045-1027). Heat treatment transforms microcrystalline nickel and Ni_xP_y phases into crystalline Ni and stable Ni_3P phase (JCPDS Ref. no.: 01-074-1384) [2]. XRD pattern of Ni–P–TiO_2 [Fig. 5b] reveals that apart from single broad peak of microcrystalline Ni, small peaks of TiO_2 (JCPDS Ref. no.: 01-071-1166) are also present. It is observed that the incorporation of TiO_2 particles into the EL Ni–P matrix shows no structural modification as the peaks corresponding to Ni and Ni_3P remains the same. Heat treatment results in crystalline phases of Ni, Ni_3P, TiO_2 and Fe. The peak of Fe (JCPDS Ref. no.: 00-006-0696) may arise from the substrate used.

The microhardness of Ni–P alloy coating is found to be 414 VHN. As expected, heat treatment increases the coating hardness upto 815 VHN. The phase transformation occurs within the coating which results in the precipitation of Ni_3P phase on heat treatment at 400 °C for 1 h [8]. The presence of Ni_3P phase improves the hardness of the alloy coatings and it can be compared as that of the hard chrome coatings. The improvement in the hardness of the coatings was noticed upto 510 VHN, when TiO_2 particles were added on as secondary phase reinforcement. The upgradation in the hardness of 90 units can be attributed toward the presence of the second phase TiO_2 particles in Ni–P matrix. The heat treatment of the nanocomposite coating enhances trait upto 935 VHN [Fig. 6a].

The effect of sliding distance on the friction coefficient of the EL Ni–P–TiO_2 coating under 0.1 N, 0.15 N and 0.20 N loads is shown in Fig. 6b. Here chromium steel ball is sliding over the specimen. The composite coatings are greatly affected by the load and rotation speed. The coefficient of friction for EL Ni–P–TiO_2 composite coating increases with the increase in sliding distance attains maximum value and then maintain at constant level. The increment in coefficient of friction with sliding distance is attributed toward the mutual contributions from the adhesion between the surfaces as well as plowing of the steel ball by hard second phase TiO_2 particles embedded in the electroless nickel matrix [13].

The dynamic coefficient of friction of Ni–P–TiO_2 composite coating increases from 0.25 to 0.7 with the increase of load from 0.1 N to 0.2 N as the real contact area between the nanocomposite coating and counterface steel ball increases with increase in load. Fig. 6c shows the effect of sliding distance on the friction coefficient of the Ni–P alloy and Ni–P–TiO_2 composite coating under 0.1 N load. The friction coefficients of the EL Ni–P–TiO_2 nanocomposite coating decreases with sliding as compared with Ni–P alloy coating and mild steel substrate. The lowest coefficient of friction accounts to highest hardness attained by heat treated Ni–P–TiO_2 nanocomposite coating due to the trapping of titania particles in the Ni–P matrix and precipitation of Ni_3P phase by heat treatment. It is also observed that with increase in rotational speed, the coefficient of friction of EL Ni–P–TiO_2 nanocomposite coatings increases [Fig. 6d]. The wear resistance of the EL Ni–P–TiO_2 nanocomposites coincides well with the microhardness of the coating. The SEM micrographs of the worn surfaces of the Ni–P matrix and Ni–P–TiO_2 nanocomposites were shown in Fig. 7. In case of Ni–P coating, the worn surface along the sliding direction is composed of longitudinal grooves and partial irregular pits. The presence of grooves indicates the micro-cutting and micro-plowing effect of the counter face, while pits are the sign of ductile fracture. On the other hand, for Ni–P–TiO_2, the worn surface seems to have wide grooves and is hard adhered

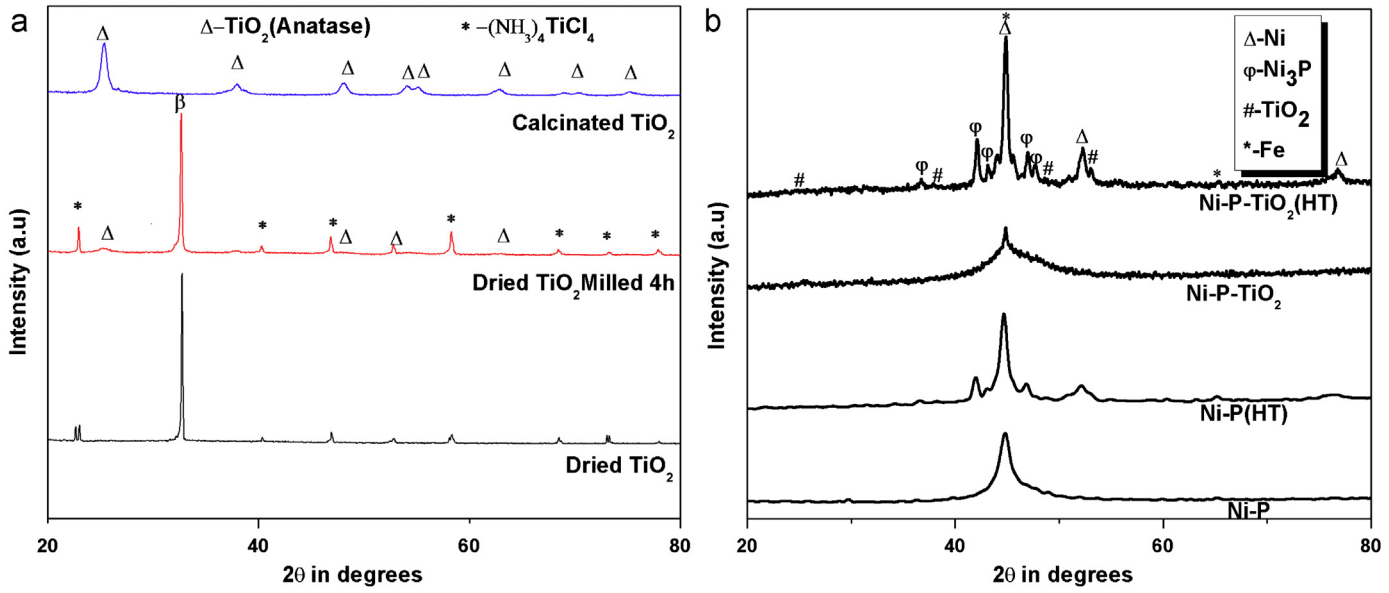

Fig. 5. XRD patterns of (a) dried TiO_2, milled TiO_2 for 4 h and calcined TiO_2 at 500 °C for 1 h; EL coatings and (b) Ni–P and Ni–P–TiO_2 in 'as coated' and heat treated condition.

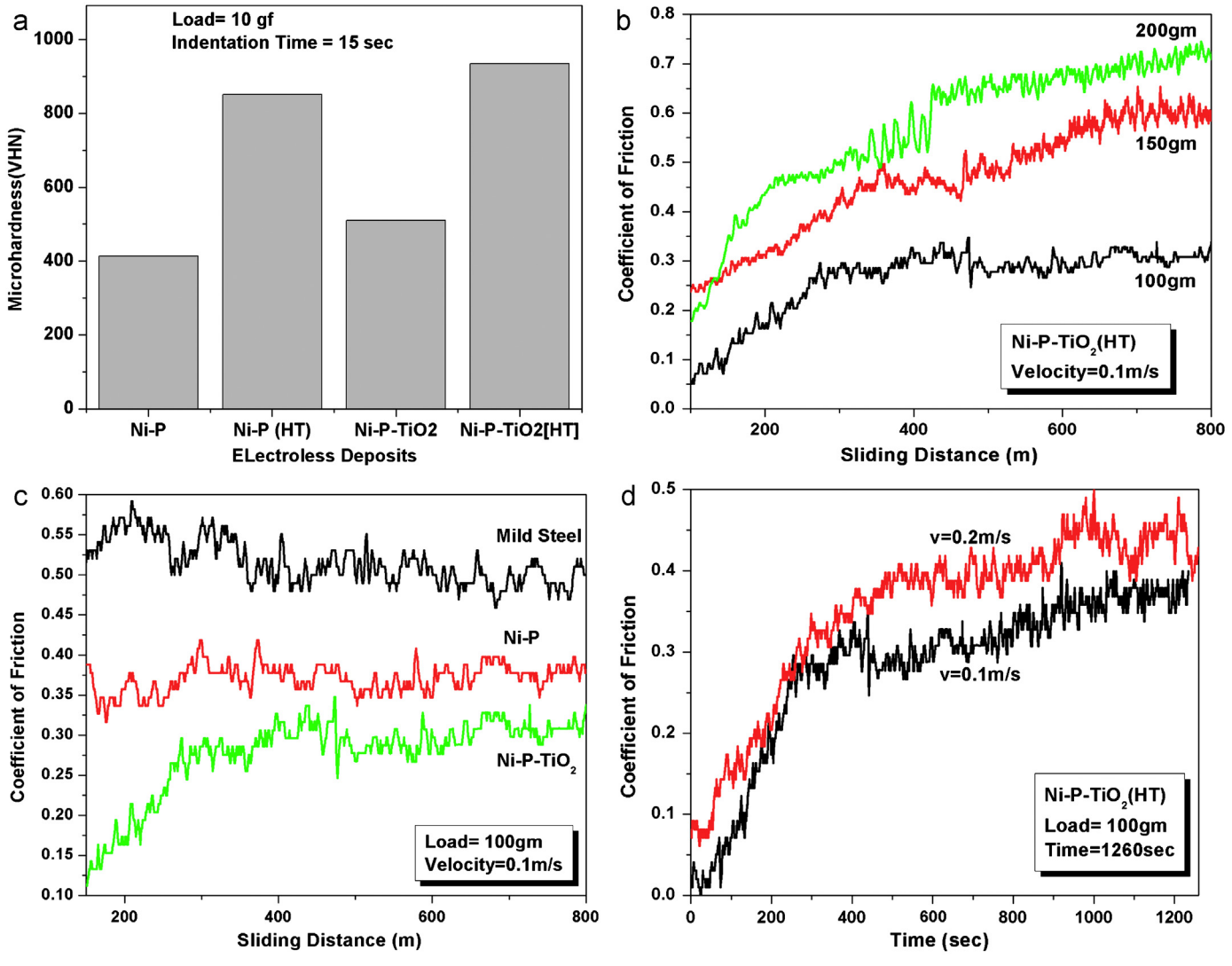

Fig. 6. Hardness of EL coatings in 'as coated' and HT condition (a) Ni–P and Ni–P–TiO_2; effect of sliding distance on the friction coefficient of (b) EL Ni–P–TiO_2 composite coating at varying loads; (c) substrate, EL Ni–P and Ni–P–TiO_2 under 0.1 N load and (d) friction coefficient of EL Ni–P–TiO_2 at varying rotation speed.

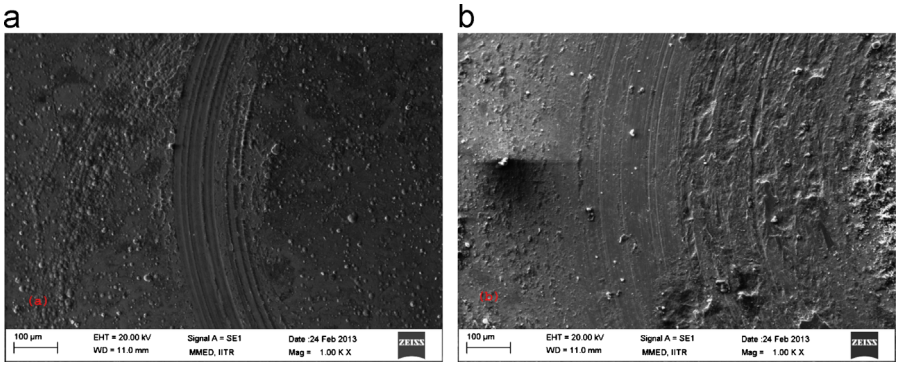

Fig. 7. SEM images of EL composite coatings after wear tests under a 0.10 N load (a) Ni–P coating and (b) Ni–P–TiO_2.

may be due to the oxidation of the surface and severe wear of the counterpart by the TiO_2 incorporated Ni–P matrix composite.

4. Conclusions

TiO_2 nanoparticles (12 nm) are synthesized by the precipitation method. Codeposition of TiO_2 into the Ni–P matrix results in surface modification of the coatings. Phase analysis of Ni–P–TiO_2 coating by XRD confirms the presence of Ni and TiO_2. Heat treatment (400 °C for 1 h) causes amorphous to crystalline Ni transformation with Ni_3P phase. Ni–P–TiO_2 nanocomposites exhibit high hardness, 935 VHN after heat treatment than Ni–P alloy coatings. The friction coefficient of Ni–P–TiO_2 nanocomposites is found to be lower than EL Ni–P coatings. The friction coefficient of Ni–P–TiO_2 nanocomposites increases with increasing load and rotational speed. Abrasive wear mechanism is involved as indicated by worn surfaces of Ni–P and Ni–P–TiO_2 coatings.

Acknowledgments

Authors are thankful to DST, UCOST for providing the research fund.

References

[1] K. Hari Krishnan, S. John, K.N. Srinivasan, J. Praveen, M. Ganesan, P.M. Kavimani, An overall aspect of electroless Ni–P depositions: a review article, Metallurgical and Materials Transactions A 37A (2006) 1917–1926.

[2] Ramesh Chandra Agarwala, Vijaya Agarwala, Rahul Sharma, Electroless Ni–P based nanocoating technology—a review, Synthesis and Reactivity in Inorganic Metal—Organic Chemistry 36 (2006) 493–515.

[3] J.N. Balaraju, T.S.N. Sankara Narayana, S.K. Seshadri, Electroless Ni–P composite coatings, Journal of Applied Electrochemistry 33 (2003) 807–816.

[4] Preeti Makkar, R.C. Agarwala, Vijaya Agarwala, Studies on electroless coatings at IIT Roorkee—a brief review, Materials Science Forum 33 (2013) 275–288.

[5] Prasanta Sahoo, Suman Kalyan Das, Tribology of electroless nickel coatings—a review, Materials and Design 32 (2011) 1760–1775.

[6] J. Novakovic, P. Vassiliou, Kl. Samara, Th. Argyropoulos, Electroless NiP–TiO_2 composite coatings: their production and properties, Surface and Coatings Technology 201 (2004) 895–901.

[7] J. Novakovic, P. Vassiliou, Vacuum thermal treated electroless NiP–TiO_2 composite coatings, Electrochimica Acta 54 (2009) 2499–2503.

[8] S.B. Sharma, R.C. Agarwala, V. Agarwala, S. Ray, Dry sliding wear and friction behaviour of Ni–P–ZrO_2–Al_2O_3 composite electroless coatings on aluminium, Materials and Manufacturing Processes, Marcel Dekkar Publication 17 (5) (2002) 637–649.

[9] S. Alirezaei, S.M. Monirvaghefi, M. Salehi, A. Saatchi, Wear behavior of Ni–P and Ni–P–Al_2O_3 electroless coatings, Wear 262 (2007) 978–985.

[10] M. Momenzadeh, S. Sanjabi, The effect of TiO_2 nanoparticle codeposition on microstructure and corrosion resistance of electroless Ni–P coating, Materials and Corrosion 63 (2012) 614–619.

[11] O.R.M. Khalifa, E. Abd El-Wahab, A.H. Tilp, The effect of Sn and TiO_2 nanoparticles added in electroless Ni–P plating solution on the properties of composite coatings, Australian Journal of Basic and Applied Science 5 (6) (2011) 136–144.

[12] Zolta´n Ambrus, Na´ndor Bala´zs, Tünde Alapi, Gyula Wittmann, Pa´l Sipos, Andra´s Dombi, Ka´roly Mogyoro´si, Synthesis, structure and photocatalytic properties of Fe (III)-doped TiO_2 prepared from $TiCl_3$, Applied Catalysis B: Environmental 81 (2008) 27–37.

[13] J.K. Dennis, K.S. Sagoo, Wear behavior of engineering coatings and surface treatments, Metal Finishing 89 (1991) (1991) 111–121.